Published in Journal of Hydrology, 288, issues 3-4, 327-343, 2004
which should be used for any reference to this work

The problem of salt recycling and seawater intrusion in coastal irrigated plains: an example from the Kiti aquifer (Southern Cyprus)

Ellen Milnes*, Philippe Renard[1]

Centre of Hydrogeology, Institute of Geology, University of Neuchâtel, Rue Emile Argand 11, CH-2007 Neuchâtel, Switzerland

Abstract

In coastal aquifers which are exploited for agricultural purposes, salinisation by salt recycling from irrigation is superimposed on the effects of seawater intrusion. Water quality degradation of irrigation pumping wells caused by seawater intrusion further enhances salinisation by irrigation, as the extracted solute mass is recycled and is not withdrawn from the system.

The main objective of this study is the investigation and quantification of the impact of solute recycling from irrigation relative to seawater intrusion. A *solute mass budget* was established by expressing the solute mass return flow as fraction of the extracted solute mass from wells by means of a *solute mass return flow ratio* (r_r). The obtained expression for the relative contribution of solute recycling from irrigation is an exponential function of the return flow ratio r_r and normalised time $\bar{t}$ only (time versus system turnover time).

This expression was applied to an example, the Kiti aquifer (Southern Cyprus), where field observations suggest that solute return flow is a super-imposed salinisation mechanism. The contribution from solute recycling normalised with the solute mass flux entering from the sea after 20 years was found to be 1.5–8.5% in the extracted solute mass flux, depending on the estimation of the system turnover time.

Subsequently, a coupled finite element model, reflecting the main features of the Kiti aquifer was used as a possible 'synthetic reality', to test the relative impact of solute recycling on the spatial salinity distribution in a complex hydrogeological and geometrical setting. This was done by running two simulation scenarios: (1) recycling all the extracted solute back into the system and (2) leaving solute recycling aside and comparing the results of these two scenarios relative to each other and to patterns observed in the field. The results showed, that by introducing solute recycling into the numerical model as coupled boundary condition does not only respect the overall solute mass balance but can have an important impact on the salinity distribution, leading to a significant spreading of the mixing zone, similar to what was observed in the field.

Keywords: Salt recycling; Solute mass budget; Seawater intrusion; Transport modelling; Irrigation salinity; Cyprus

* Corresponding author. Tel.: +41-32-718-27-59; fax: +41-32-718-26-03.
E-mail addresses: ellen.milnes@unine.ch (E. Milnes), philippe.renard@unine.ch (P. Renard).
[1] Tel.: 41-32-718-25-37; fax: 41-32-718-26-03.

1. Introduction

In numerous coastal aquifers, particularly in semi-arid and arid regions, over-exploitation has led to

groundwater quality degradation. As a consequence seawater intrusion has been intensively studied for several decades (see Bear et al., 1999 for a recent synthesis). The growing demand in groundwater resources is mostly linked to an intensification of agricultural activity, which is very dependent on water from irrigation. In this work we focus on the effects of seawater intrusion combined with the superimposed effects of groundwater quality degradation related to solute recycling from irrigation. The salinisation mechanisms governing seawater intrusion and solute mass return flow from irrigation are very different, but they are coupled by the fact that the water quality degradation observed in pumping wells, initially caused by seawater intrusion as a consequence of landward directed hydraulic gradients, is further enhanced by salinisation due to solute return flow from irrigation. Since the potential remedial measures are very different for seawater intrusion settings as opposed to irrigation return flow affected areas, it is important to distinguish between the two salinisation mechanisms and to understand how they are linked. Many geochemical techniques have been developed to identify different origins of salinity in coastal contexts, but they are often equivocal (Vengosh and Rosenthal, 1994; Vengosh et al., 1999, 2002; Kolodny et al., 1999; El Alcheb et al., 2001; Kim et al., 2003).

The physics of seawater intrusion are rather well understood and numerical modelling approaches, using sophisticated software packages allowing density-dependent flow and transport simulations, are regularly used as tools to evaluate future salinity evolutions or for optimisation purposes (Essaid, 1990; Xue et al., 1995; Gambolati et al., 1999; Voss, 1999; Gordon et al., 2000; Oude Essink, 2001; Paniconi et al., 2001). Unfortunately, in many cases the model applications are limited, on the one side, by the data availability, and on the other side, by the fact that, even under extremely controlled conditions, when all the physical properties of the medium are independently measured, the numerical models require a very fine discretisation to reproduce the results of physical experiments accurately (Johannsen et al., 2002). This shows rather clearly the limitations of what one could expect in a complex natural system when the geometry, the physical parameters, and the boundary conditions are not well defined.

Looking at the other side of the problem, groundwater quality degradation due to solute mass return flow from irrigation has received a lot of attention, particularly in the United States and Australia, in areas far from the sea. Authors such as Konikow and Person (1985), Bouwer (1987), Close (1987), Beke et al. (1993), and Prendergast et al. (1993) have focused on the establishment of solute mass budgets and on the quantification of the mechanisms of groundwater salinisation by the solute mass loading of the unsaturated soil due to irrigation practices and subsequent flushing and transfer to the groundwater body. Salinities up to 10 mS/cm can often be found in areas where mismanagement and poor irrigation practices have led to groundwater deterioration.

The main objective of the present work is the investigation of the importance of salt recycling from irrigation relative to seawater intrusion based on an analysis of the behaviour of a *solute mass budget* as function of *solute mass return flow* from irrigation. A pertinent reason for evaluating the contribution of solute recycling from irrigation, is if a long-term numerical flow and transport approach is envisaged. What we will call ‘the classical numerical approach’ used in seawater intrusion settings does not introduce solute mass return flow from irrigation as a coupled boundary condition, being a function of the extracted solute mass flux from the well boundary conditions. To give an example of a ‘classical numerical approach’, Sherif and Hamza (2001) discussed the possibility of mitigating seawater intrusion by pumping brackish water and using it for irrigating certain crops or developing green lands. In a two-dimensional vertical model, the effect of pumping in the brackish mixing zone led to a reduction of the dispersion of the mixing zone width. This is certainly true for the case where the pumped water is not used for irrigation but removed from the system (e.g. rejection back to the sea), but if it is supposed to be used for irrigation within the modelled system as suggested, it reflects a modelling approach, which does not comply with the true solute mass balance. Therefore, what we call the classical numerical approach yields ‘best-case’ results, since it removes all the extracted solutes from the system. The reason why solute return flow from irrigation is not included in flow and transport models is that the physical

process of solute re-distribution from pumping wells onto the fields is a man-made process, beyond the flow and transport equations. Sometimes numerical approaches of seawater affected areas do include fluid return flow from irrigation (Paniconi et al., 2001), but making the assumption that no solute recycling takes place. Others assign a fixed value to the contribution from irrigation solute return flow, in which case the assigned value is not a function of the solutes extracted from well-boundary conditions (Voss, 1999).

The paper is subdivided into three main sections. In the first part, we develop a simplified transient solute mass budget, based on long-term average (steady state) flow conditions. In the second section, an example from a coastal area in Cyprus, the Kiti aquifer, is presented. A field assessment of the salinisation combined with interpretation of historical data suggested that salt recycling is a superimposed important salinisation mechanism in the area, where agricultural activity is intensive. The impact of solute recycling is then assessed by the analytical expression established in the first section. In the third part, a coupled finite element flow and transport model is used for the purpose of testing the impact of solute return flow on the spatial salinity distribution in a complicated hydrodynamic and geometrical context.

2. Solute mass budget

In over-exploited coastal aquifers, most of the extracted water used for irrigation leaves the system by means of evapo-transpiration. The solutes remain and are concentrated within the unsaturated zone before they are leached and transported to the groundwater again when the soil is flushed by percolation of precipitation. The only possible losses of solutes in coastal aquifers are to the sea and export of extracted water (e.g. water supply), being the two main system outlets. However, export of extracted groundwater is done for water with low solute contents and is therefore not an important salt sink, and in over-exploited aquifers the sea is more of a recharge area than a discharge area and is thus a source of salinisation, not a sink. Hence, the more a coastal aquifer is salinised, the less salt is exported and therefore, over-exploited coastal aquifers can be considered as solute traps.

In this section, our aim is to consider the over-exploited aquifer as a closed system and to evaluate the contribution of solute return flow to the overall salinisation (solute mass) of the system.

We make the assumption that the aquifer of interest is exploited in a regime of equilibrium with respect to flow. In other words, if only the fluxes of water are considered, the aquifer has reached steady state in which the reserves are not varying and pumping is fully compensated by the inflow from recharge and from seawater intrusion. Such a hypothesis can only be supported, if the chosen steady-state condition is based on long-term averages, and if the variations of the reservoir storage over the chosen long-term period can be neglected.

In the following, the aquifer is not discretised and therefore an average concentration $C(t)$ representing the 'perfect system mixture' of the entire aquifer will be considered. Even though we are aware of the fact, that operating with an average concentration does not provide any result in itself concerning the spatial solute distribution, it has been found very useful in isolating the contribution of solute return flow from irrigation from the salinisation effect due to seawater intrusion.

Assuming perfect mixing, the solute mass conservation can be written as the balance between the in-flowing and the out-flowing components

$$\frac{\partial(\phi VC)}{\partial t} = \sum q_{\text{in}} c_{\text{in}} - \sum q_{\text{out}} C + S \tag{1}$$

where C [ML^{-3}] represents the mean concentration of the system, ϕ [−] the porosity, V [L^3] the volume of the aquifer, $q_{\text{in/out}}$ [L^3T^{-1}] the fluid mass fluxes, c_{in} the respective inflowing concentrations [ML^{-3}] and S [MT^{-1}] the sources and sinks. The specific components of Eq. (1) in a coastal environment are defined and shown in Fig. 1.

We then define a solute mass return flow ratio r_{r} [−] as the ratio of the solute mass flux entering the system by return flow versus the extracted solute mass flux from wells

$$r_{\text{r}} = \frac{q_{\text{rf}} c_{\text{rf}}(t)}{q_{\text{p}} C(t)} \tag{2}$$

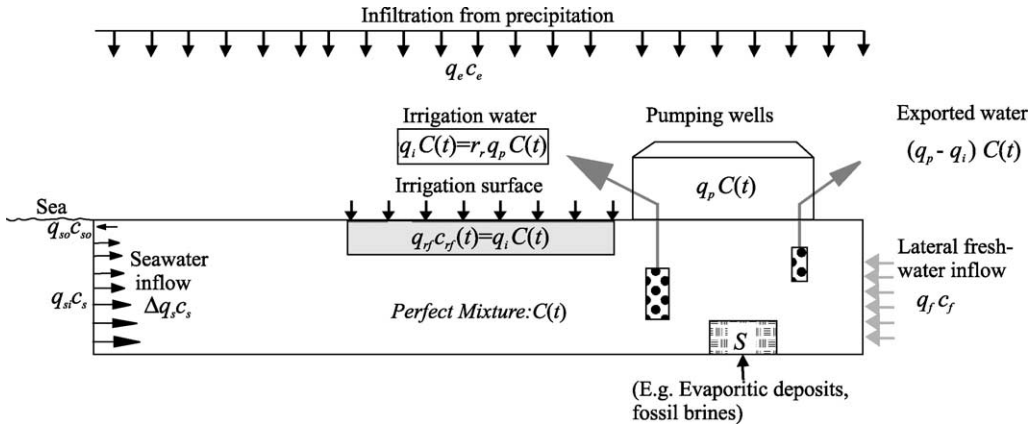

Fig. 1. Schematic illustration of flow components and their respective concentrations. For average (steady state) flow conditions, the sum of the in and out going flow rates equal zero. Both the sea and freshwater concentrations are considered as time-invariant.

with q_{rf} representing the vertical flux of water which percolates down to the groundwater below irrigated surfaces; $c_{rf}(t)$, the corresponding concentration; q_p, the extraction rate; $C(t)$ is the concentration of the extracted fluid. For $r_r = 0$, all the extracted solute mass is exported from the system, and for $r_r = 1$, the entire extracted solute mass is recycled.

Since $c_{rf}(t)$ in Eq. (2) is usually unknown, another equivalent definition is required to determine r_r. Defining q_i as the amount of the extracted fluid flux q_p which is not exported out of the system, thus representing the part used for irrigation (with $C(t)$ being its concentration), another expression can be found for r_r. Since the solute mass flux $q_i C(t)$ applied for irrigation is equal to the solute mass flux which will be recycled into the aquifer system, replacing q_{rf} $c_{rf}(t)$ in Eq. (2) by $q_i C(t)$ yields

$$r_r = \frac{q_i}{q_p} \tag{3}$$

The return flow ratio is thus defined as the proportion of extracted fluid flux used for irrigation (containing the solute mass which will be recycled to the system) relative to the total extracted fluid flux. This quantity can usually be estimated fairly well in irrigated aquifers, thus allowing determination of r_r.

According to the definition of r_r, we can express the solute mass flux derived from return flow $m_{rf}(t)$ by means of the extracted solute mass flux as follows:

$$m_{rf}(t) = q_i C(t) = r_r q_p C(t) \tag{4}$$

The other terms in Eq. (1) are characterised by time-invariant known concentrations (Fig. 1). Along the coastline, and due to the fact that we are considering an over-exploited aquifer, we assume that the balance of the fluxes $\Delta q_s = (q_{si}\text{-}q_{so})$ is always positive and that $q_{si} \gg q_{so}$, with q_{si} being the seawater flux entering the system along the shoreline and q_{so} the fluid flux leaving the system along the shoreline. Therefore, the concentration of Δq_s is close to seawater concentration and will be approximated in the following by seawater concentration c_s, which will lead to a slight underestimation of the entering solute mass flux. The lateral freshwater inflow q_f has a mean freshwater concentration c_f and finally, the effective vertical infiltration q_e is given the concentration of rainwater c_e. All the above-mentioned constant components can be used to define the total constant incoming solute mass flux (m_i) as follows:

$$m_i = \Delta q_s c_s + q_f c_f + q_e c_e \tag{5}$$

Making use of Eqs. (4) and (5) the in-flowing and out-flowing components in Eq. (1) can be written as follows

$$\text{in}: \quad \sum q_{in} c_{in}(t) = m_i + m_{rf}(t) = m_i + r_r q_p C(t) \tag{6}$$

$$\text{out}: \quad \sum q_{out} C(t) = q_p C(t) \tag{7}$$

For reasons of simplicity the source term in Eq. (1) will be left aside, although it can be added at any time.

Combining Eqs. (6) and (7) allows us to reformulate Eq. (1) as follows

$$\frac{\partial C}{\partial t} = \frac{1}{\phi V}[m_i + (r_r - 1)q_p C(t)] \quad (8)$$

for which the solution with initial condition $C(0) = 0$ is:

$$r_r < 1,\ C(t) = \frac{m_i}{q_p(1-r_r)}\left[1 - e^{-((q_p(1-r_r)t)/\phi V)}\right] \quad (9)$$

$$r_r = 1,\ \ C(t) = \frac{m_i}{\phi V}t \quad (10)$$

For a return flow ratio $r_r = 1$ the concentration will increase linearly with time.

Still making the hypothesis that the well extractions are the only exiting fluxes, the system turnover time t_0 being the ratio of the porous volume to steady flow rate reads

$$t_0 = \frac{\phi V}{q_p} \quad (11)$$

Introducing t_0 into Eq. (9) and defining the ratio t/t_0 as $\bar{t}$ leads to the following expressions for the mean system concentration after reformulation

$$r_r < 1,\ \ C(\bar{t}, r_r) = \frac{m_i}{q_p(1 - r_r)}[1 - e^{-\bar{t}(1-r_r)}] \quad (12)$$

$$r_r = 0, \qquad C(\bar{t}) = \frac{m_i}{q_p}[1 - e^{-\bar{t}}] \quad (13)$$

For values of $r_r < 1$ the concentration of Eq. (12) will tend towards an asymptotic steady-state concentration at infinity which equals the ratio between the constant incoming solute flux m_i and the exported fluid flux $q_p(1 - r_r)$:

$$C(\infty) = \frac{m_i}{q_p(1 - r_r)} \quad (14)$$

Eq. (13) describes the mean system concentration evolution for the case that no recycling takes place. When comparing it to Eq. (12) one can see that $C(\bar{t}, r_r)$ will always be higher in the case of existing recycling than for the case $C(\bar{t}, r_r = 0)$.

We define $m_{pr}(\bar{t}, r_r)$ as the solute mass flux extracted from pumping wells originating from solute return flow from irrigation. To estimate it, we simply make the difference between the total solute mass flux $C(\bar{t}, r_r)q_p$ and the solute mass flux if no return flow takes place $C(\bar{t}, r_r = 0)q_p$. The contribution of solute recycling can then be expressed as follows:

$$m_{pr}(\bar{t}, r_r) = C(\bar{t}, r_r)q_p - C(\bar{t}, r_r = 0)q_p \quad (15)$$

Using Eqs. (12) and (13) and normalising $m_{pr}(\bar{t}, r_r)$ with m_i, the following expression can be written for the relative contribution of solute recycling $\bar{m}_{pr}(\bar{t}, r_r)$ to the overall extracted solute mass flux, being a function of the normalised time $\bar{t}$ and the return flow ratio r_r only

$$\bar{m}_{pr}(\bar{t}, r_r) = \frac{m_{pr}(\bar{t}, r_r)}{m_i} = \frac{1}{(1-r_r)}[1 - e^{-\bar{t}(1-r_r)}] - [1 - e^{-\bar{t}}] \quad (16)$$

Fig. 2 is the graphical representation of Eq. (16) for a range of different return flow ratios. If the turnover time t_0 is known, the relative contribution of solute return flow $\bar{m}_{pr}(t)$ can easily be deduced for any characteristic time t of interest (e.g. simulation time-span, exploitation time-span) and return flow ratio r_r. It reveals, that the relative contribution of solute return flow $\bar{m}_{pr}(\bar{t}, r_r)$ increases with increasing r_r and increasing $\bar{t}$. In other words, for one and the same extraction rate and return flow ratio, but for different reservoir sizes, the smaller reservoir with a shorter turnover time will be more affected by solute return flow from irrigation, since $\bar{t}$ is bigger. On the other hand, for the same size reservoir and extraction rate, an increasing return flow ratio r_r will increase the impact of solute return flow from irrigation.

The relative impact of solute recycling is thus completely conditioned by the ratio of the characteristic time t relative to the mean system turnover time t_0, and by the return flow ratio r_r.

3. An example from Southern Cyprus: the Kiti aquifer

At this point we would like to present a case study carried out in Southern Cyprus, which initially triggered this investigation of the importance of solute mass return flow from irrigation as a potential superimposed coupled mechanism to salinisation of

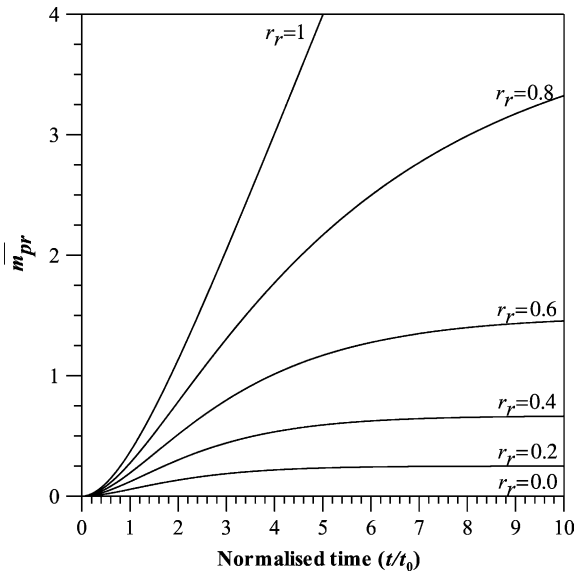

Fig. 2. Graphical representation of Eq. (16) with the dimensionless time $\bar{t}$ (t/t_0) as x-axis versus the relative contribution of solute return flow from irrigation $\bar{m}_{\mathrm{pr}}(\bar{t}, r_{\mathrm{r}})$. This dimensionless graphic is valid for any system for which the formulated assumptions are valid.

coastal aquifers. The assessment of the spatial and temporal behaviour of the salinity distribution within the aquifer revealed that the smaller the saturated thickness and the more intensive agricultural activity was, the wider was the mixing zone. This observation was not directly interpretable within the usual seawater intrusion paradigm and led to this quantitative investigation of the importance of solute return flow from irrigation. In this section we present an overview of the field observations and then apply the solute mass balance approach elaborated in Section 2 to evaluate the potential impact of solute recycling for the Kiti aquifer.

3.1. Hydrogeological context

The Kiti aquifer is situated in the east of Southern Cyprus, south of Larnaca (Fig. 3), an area with a semi-arid climate, forming a plain with elevations reaching up to 20 masl in the north and with a surface area of approximately 30 km^2.

In the Kiti aquifer, as in numerous coastal aquifers, over-exploitation has led to groundwater quality degradation during the past decades. Locally, over-exploitation temporarily diminished the hydraulic head by as much as 12 m below sea level in the early 80 s, leading to pronounced landward directed gradients, and thus to an acceleration of seawater intrusion.

Groundwater abstraction, mainly for irrigation, was an average of 3×10^6 m^3/year up to 1981,

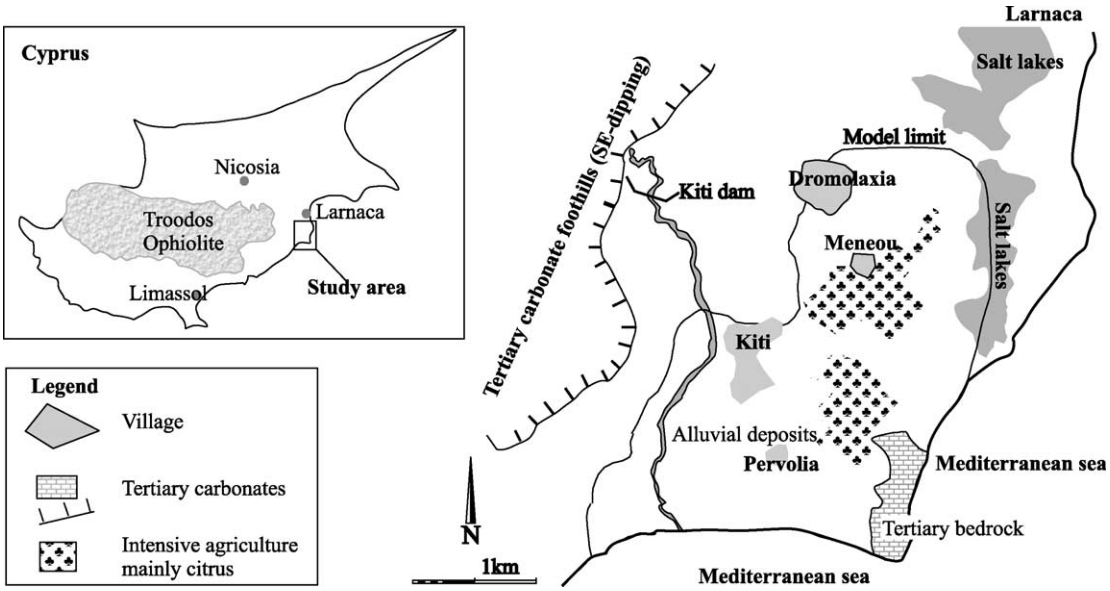

Fig. 3. Main physiographic features of the Kiti area, Southern Cyprus, showing the limit of the Kiti aquifer with respect to the sea, the main villages, the most important agricultural areas, the salt lakes and the outcropping bedrock (carbonates).

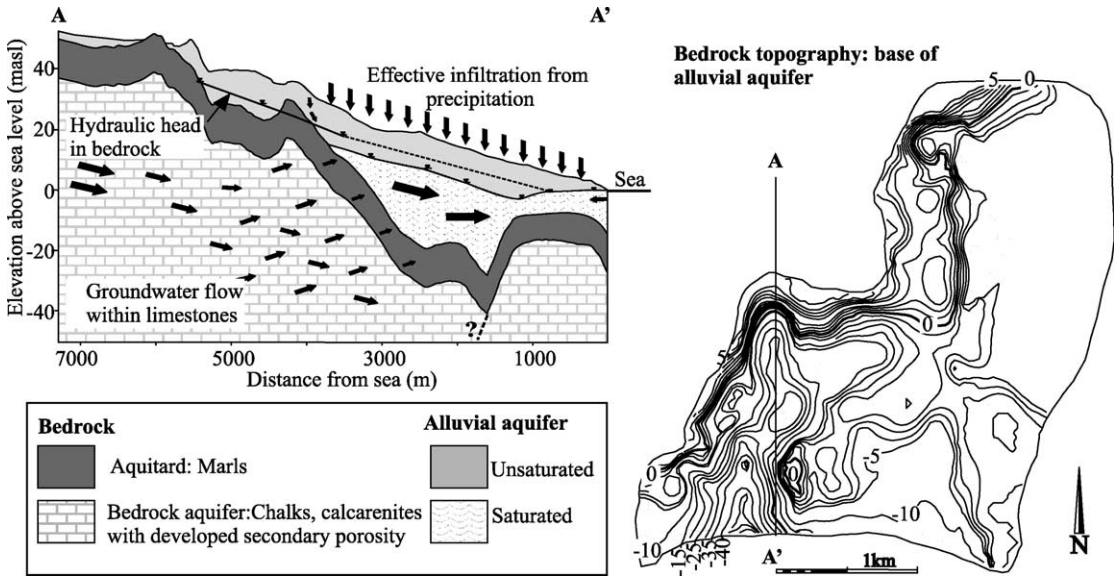

Fig. 4. Simplified geological N–S-cross-section through the Kiti aquifer system visualising the conceptual model based on geologic and hydrodynamic data. The bedrock topography or base of the alluvial aquifer is shown, revealing the prominent Miocene NS-oriented paleo-channel in the west.

but was subsequently reduced to 1.8×10^6 m^3/year by the mid 90 s and to $1.3–1.5 \times 10^6$ m^3/year in recent years. The water table recovered somewhat in the 90 s but is still below sea level during the main pumping season.

The shoreline forms the southern and, partially, the eastern boundary of the aquifer, while two salt lakes are situated in the northeast. The aquifer system is layered, consisting of an upper, unconfined, alluvial aquifer separated from a lower, confined carbonate aquifer by Pliocene marls (Fig. 4), a similar hydrogeological setting as presented by Frind (1982). The inland aquifer limit was defined as the area within which the alluvial aquifer is saturated. The position of the bedrock was deduced from borelog records and geophysical data. The saturated thickness of the unconsolidated alluvial aquifer ranges from 3 to 10 m in the east to a maximum of 50 m in the west, where a Miocene paleo-erosional surface of the Thremithos River has formed a gully shaped channel in the bedrock. Fig. 4 shows an idealized N–S geological cross-section through the Kiti aquifer system, with indicated zones of potential drainage from the carbonate aquifer towards the alluvial aquifer and also the areas where the alluvial aquifer is saturated. The Miocene NS-directed paleo-channel of the Tremithos River can be clearly seen in the bedrock topography.

Annual recharge by infiltration of precipitation and subsurface inflow was estimated to be an average of $1.8–2.5 \times 10^6$ m^3/year for the 1980s (Schmidt et al., 1988).

3.2. Assessment of salinisation

To characterise the seawater intrusion in the Kiti aquifer, historical chloride data were compared to the established time-equivalent piezometric maps. The most pronounced hydraulic depressions were found to be situated in the west, in the area of the paleo-channel, whereas the most prominent salinity anomalies were generally observed in the central zone. Fig. 5 shows the distribution of the electrical conductivity as derived from 76 measurements taken at depths of approximately 3–5 m below the water table in open wells within the alluvial aquifer. In the area of the Tremithos paleo-channel, the seawater intrusion has advanced far inland and the salinity iso-contours indicate a relatively narrow transition

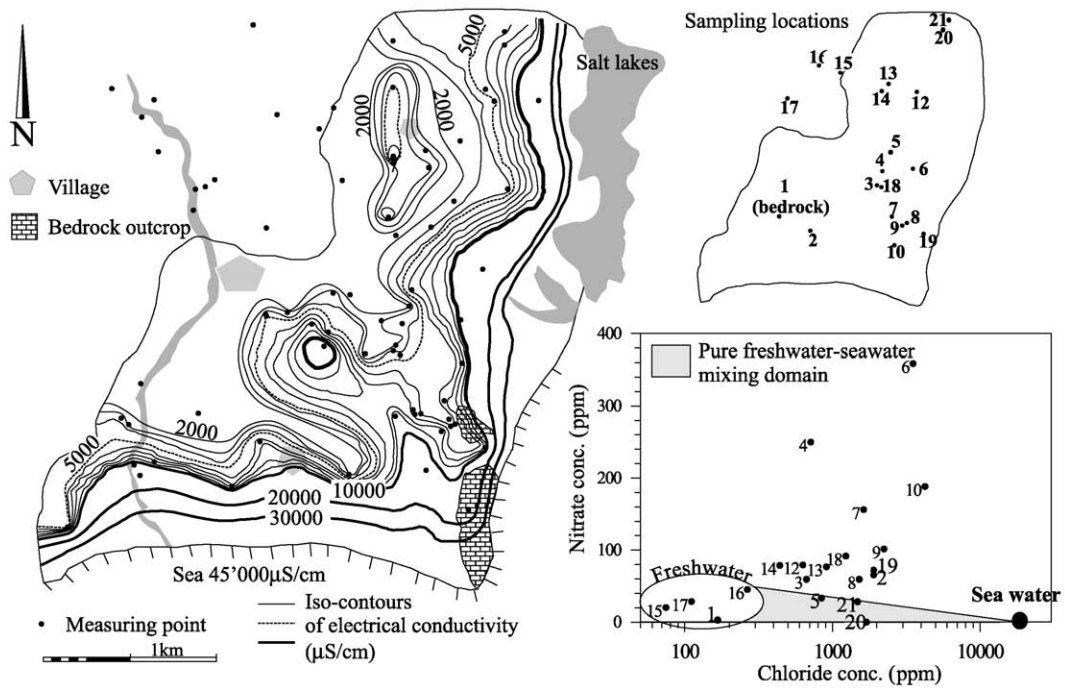

Fig. 5. Electrical conductivity distribution as derived from 78 measurements (black dots) in the alluvial aquifer (May 2001). NO_3 versus chloride concentrations are shown with chloride concentrations on a logarithmic scale. The nitrate concentrations are positively correlated in the central plain with the chloride concentrations. The area of pure seawater–freshwater mixing is indicated, and can be seen to exclude most of the samples.

zone between the seawater and the freshwater. In the central area, where the saturated alluvial aquifer thickness is only a few meters and agriculture is intensive, a large tongue-like anomaly reaches 3 km inland. In this area, a high salinity anomaly (exceeding 10 mS/cm) is laterally disconnected from the seawater front. Most of the central area is characterised by electrical conductivities between 2 and 6 mS/cm and the transition is blurred. The salinity distribution appears patchy with locally high variations. Note that pumping wells used for irrigation in the entire area are not abandoned until the electrical conductivities exceed 5–8 mS/cm. Agricultural re-distribution of the solute mass on fields goes hand in hand with the addition of nutrients (mostly nitrates) and pesticides. Sampling for chemical analysis (major ions) was done in 20 wells in the area. The results revealed a prominent impact of agriculture in all the samples taken within the central plain, with nitrate concentrations reaching up to 360 ppm. A positive correlation between chloride and nitrate concentration can be seen on Fig. 5, a feature that cannot be explained by pure mixing of the two end-members (seawater–freshwater). Evaporation of irrigation water leads to a mass loading within the unsaturated zone which is subsequently flushed and leached during heavy rainfall events (Stigter et al., 1998; Sites and Kraft, 2000; Pearce and Schumann, 2001).

These indications support the hypothesis that solute mass return flow from irrigation is a vertical salinisation mechanism superimposed on to the lateral seawater intrusion process, even though other salinity sources cannot be completely excluded. However, the existence of geogenic salt sources, typically being Messinian deposits in the Mediterranean area (Hsü et al., 1973), have most probably been eroded in the Kiti area, since they are not found in any of the borelog records and they do not crop out in the catchment of the Kiti aquifer. A geochemical survey in the region carried out by Ploethner et al. (1986) does not clearly reveal any characteristic water facies related to

evaporitic deposits but mentions the possible existence of fossil brines.

3.3. Evaluation of solute return flow component in the Kiti aquifer

According to Eq. (16), we can estimate the potential impact of solute return flow from irrigation for the Kiti aquifer. The mean system turnover time t_0 and the return flow ratio r_r had to be estimated first. In the Kiti aquifer, an average of 90% of the average extracted water q_p has been and is used for irrigation purposes, only a few water supply wells are situated further inland (10%). Assuming that the irrigation techniques are sufficiently optimised that run-off can be neglected, we can estimate the return flow ratio to be $r_r = 0.9$. The saturated aquifer volume (V) for the entire aquifer-aquitard system was found to be app. 8×10^8 m^3, as derived from the constructed three-dimensional (3D) body, with a porosity (ϕ) in the range of 8–20%, being an estimated average value for the combination of the overlying silt-clay-rich sandy, gravely deposits and the underlying marls and limestones (Höltin, 1996). The mean system porosity is the most sensitive parameter, since it significantly influences the system turnover time t_0, and therefore it is better to define a porosity range rather than fixing a single value. The average extraction rate q_p for the past 20 years has been approximately 1.5×10^6 m^3/year, leading to a mean system turnover time of 42–100 years. Introducing these values into Eq. (16) for $t_0 = 42$ years and $t_0 = 100$ years and a return flow ratio $r_r = 0.9$ provides a bandwidth for the relative temporal impact of solute return flow (Fig. 6). The sensitivity of this approach with respect to the estimation of the mean turnover time can be seen. Doubling the reservoir (by doubling the porosity) reduces the relative impact of solute return flow exponentially with time. For the time-span we are interested in simulating in the following (20 years), the relative impact of solute return flow can be seen to lie between 1.5 and 8.5% of the entering solute mass flux. This can be very significant in terms of absolute concentrations, depending on the absolute value of m_i.

If, on the other hand, we are interested in evaluating whether the observed salinity distribution in the field is partly related to solute recycling we can consider a 50 year-span, which corresponds to the time that the aquifer has been heavily exploited. For this time-length, the contribution from solute return flow from irrigation lies between 8 and 42%, if the average extraction rate used in the solute mass budget is representative for the past 50 years. In the Kiti aquifer, however, the average extraction rate for the past 50

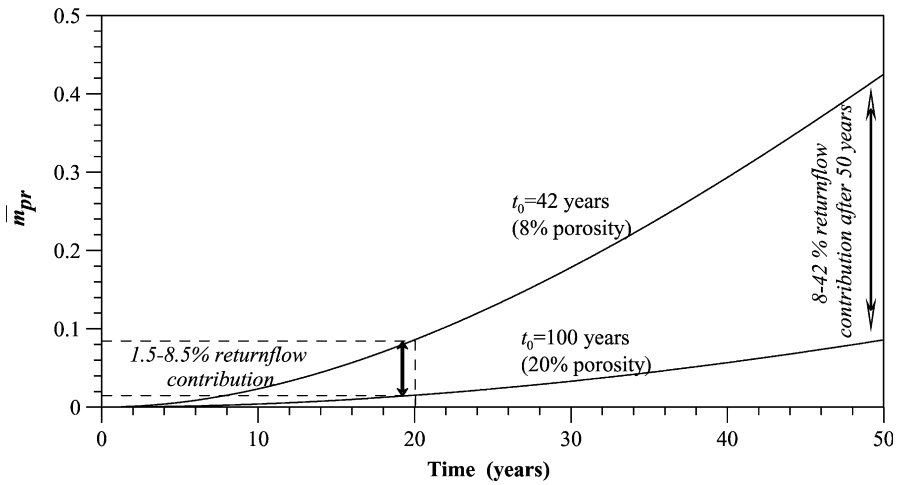

Fig. 6. Evaluation of relative solute return flow contribution $\bar{m}_{pr}$ in the Kiti aquifer based on the average extraction rates of the past 20 years for a range of estimated average system porosity (8–20%). After 20 years the relative contribution can be seen lie between 1.5 and 8.5% of the solute mass flux entering from the sea. Projection to 50 years (corresponding to historical exploitation time-span) indicates, that 8–42% of extracted solute mass flux is potentially derived from recycled solute mass, depending on the estimated mean porosity.

years is higher than for the past 20 years, which suggests an even more pronounced impact of return flow from irrigation than what was determined above. According to this evaluation, the salinity distribution observed in the Kiti aquifer is likely to be related to both seawater intrusion and solute recycling from irrigation.

4. Density-dependent flow and transport simulations

Based on the field investigations and historical data as well as former work carried out in the area (Jackovides et al., 1982; Schmidt et al., 1988), a coupled finite element flow and transport model was established, reflecting the conceptual model of the Kiti aquifer (Fig. 4). The finite element code FEFLOW (Diersch, 1998) was used to build the 3D model of the Kiti aquifer.

In the following, a description of the model and its boundary conditions will be given. Even though the parameter distribution is a result of a calibration procedure, it is very likely that the model suffers from non-uniqueness. We therefore used the model as a possible 'synthetic reality' to carry out transient flow and transport simulations for a 20-year period using the identical model for two different scenarios: (1) including solute return flow from irrigation, $r_r = 1$; and (2) without solute recycling, $r_r = 0$ being the classical numerical approach. This was done with the aim of testing the relative effect of the two extreme solute return flow ratios on the spatial salinity distribution in a complicated hydrodynamic and geometrical context. Introducing solute recycling from irrigation into a numerical model implies definition of a coupled mass boundary condition (solute return flow on irrigated plots) which depends on the time-variable cumulated solute mass flux extracted from the system by the wells, which complicates the simulation procedure.

The results from the transport simulations are then qualitatively compared to the field observations and suggest that solute return flow from irrigation is likely to be the reason for the important spreading of the mixing zone in the central area, where agricultural activity is intensive and the saturated thickness of the aquifer is small.

4.1. Boundary conditions and parameters

4.1.1. Flow boundary conditions and parameters

Along the northern limit, a lateral flux boundary condition was imposed within the bedrock aquifer, corresponding to the recharge from infiltration of precipitation on upstream outcropping carbonates Depth-dependent equivalent freshwater head boundary conditions were imposed along the seashore. The eastern boundary leads through salt lakes to the north. On the surface of the salt lakes, an out-going flux boundary condition was assigned, mimicking intensive evaporation. The mean effective infiltration was estimated on a monthly basis with the Thorntwaite method, and the annual mean value is comparable to an earlier estimation of effective infiltration in the Kiti area, carried out by Schmidt et al. (1988). The pumping wells were implemented within the alluvial aquifer (shallow wells) as extraction nodes. All other limits were defined as no flow boundaries (Fig. 7).

Average values for effective infiltration, lateral water inflow, extraction rates and observed water tables for the time-span 1994–1997 were used to calibrate the hydraulic conductivity distribution. A steady-state analysis could be carried out since the trend of the water-table showed that the storage of the system did not change significantly during this time-period. Manual adjustment of the average heads of 30 observation points according to geological criteria was followed by inverse modelling, using the Pest algorithm. Seventeen different hydraulic conductivies were adjusted. Comparing this to only 30 observation points makes it clear, that the obtained parameter distribution is likely to be non-unique, but does reflect a possible reality. Transient calibration was then carried out with the K-values as derived from the steady-state calibration to obtain the storage coefficients. For this purpose the averaged values of the same time-period 1994–1997 were decomposed into monthly values, leading to time-dependent functions for the precipitation, extraction rates and subsurface inflow.

The reliability of the model cannot be evaluated, since no sensitivity study was carried out. Indeed, and once again, we were interested in using the numerical model as a possible 'synthetic reality', reflecting the conceptual model of the Kiti aquifer

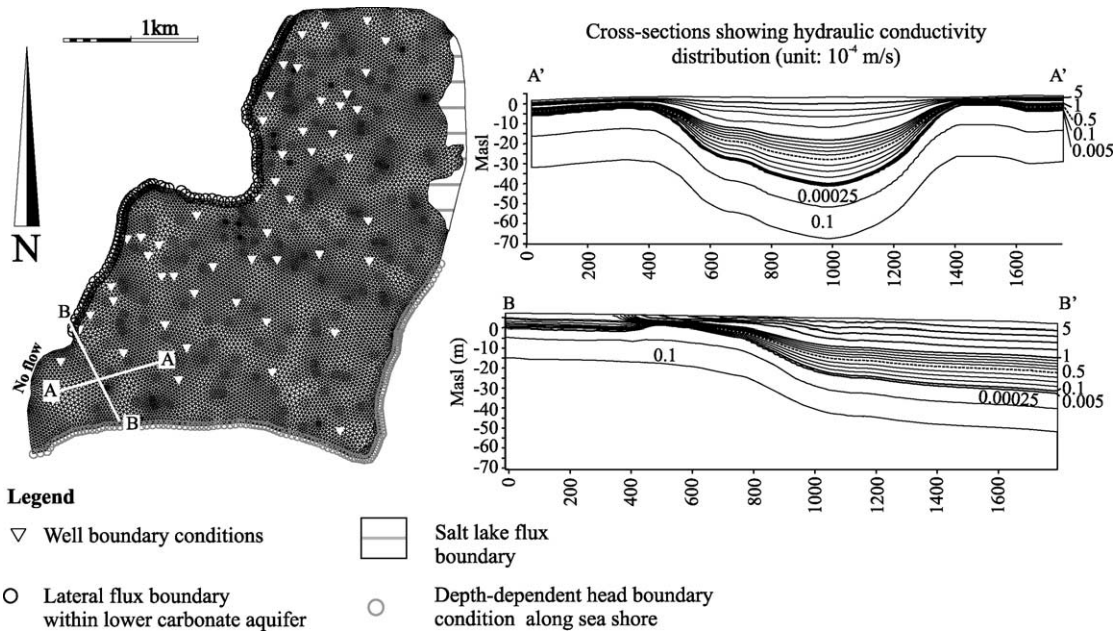

Fig. 7. Plan view of boundary conditions and finite element mesh (vertically discretised into six layers). The two cross-sections illustrate the parameter distribution as obtained from inverse modelling.

with a hydrodynamic and geometrical complexity typical of real aquifers.

4.1.2. Transport boundary conditions and parameters

Relative chloride concentrations were imposed along the shoreline (concentration $C_{\max} = 1$) and the relative northern boundary concentration was kept at $C_{\min} = 0$. The coefficient of longitudinal dispersivity (α_L) was fixed to the same order of magnitude as the cell sizes (35 m) due to the lacking knowledge of the physical value of α_L, whereas the transversal dispersion (α_T) was defined as 10% of the longitudinal dispersion.

The porosity distribution used for all simulations was attributed according to the three main geological units: porosity 10% for the alluvial heterogeneous deposits, 5% for the aquitard and 3% for the carbonates. This porosity distribution leads to a volume average of 8% for the entire aquifer, which is believed to be a rather low estimate and therefore it was used as lower boundary of the porosity range tested in the evaluation of the solute return flow in Section 3.3.

The initial concentration distribution for the two scenarios was identical and was obtained as a result of a 20-year density-dependent transport simulation run using the average hydraulic situation between 1985 and 2001 to create a shape of the seawater intrusion which was qualitatively comparable to what was observed in the early 1980s.

The only difference between the two simulation scenarios lies in a coupled areal solute mass boundary condition, introduced only for the scenario with solute return flow. The solute mass return flow from irrigation was calculated from the cumulated extracted solute mass flux from the wells at the end of each year for each square kilometre, and subsequently re-introduced as source term in the first layer of the respective square kilometres. The graph on the bottom left of Fig. 8 shows the mass of salt extracted annually from the wells (dashed line) and the annually re-introduced solute mass (solid line). The delay of one year can be seen. Leaching and solute mass return flow is believed to take place when percolation down to the groundwater after heavy rainfall takes place. A re-introduction period of 10 days was defined with a constant mass input signal. This is not based on a well defined/observed physical process, but on the assumption that the accumulated solute mass within

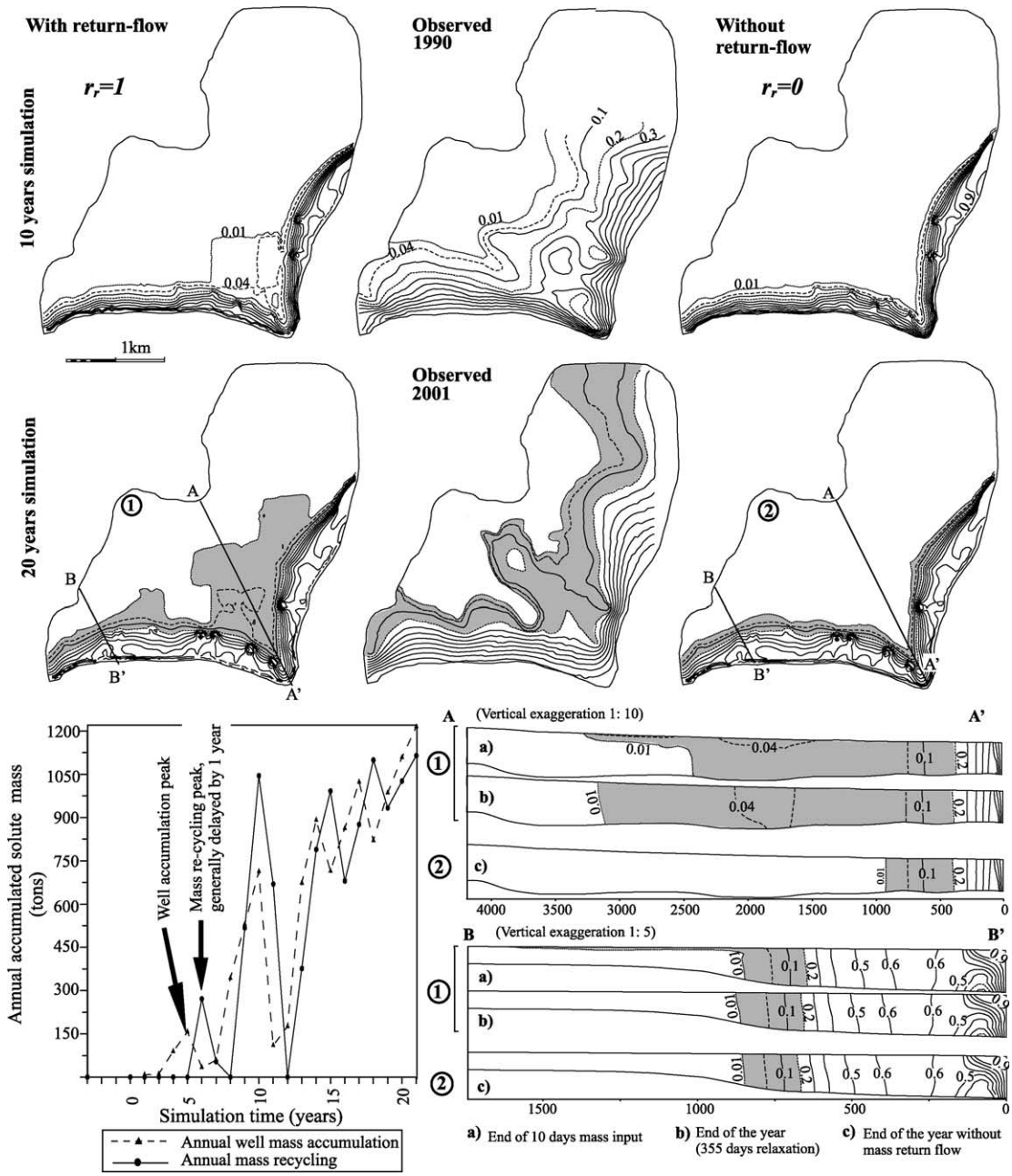

Fig. 8. Results of the numerical simulations, showing the relative mass distribution after 10 and 20 years, respectively, for the two scenarios with (left) and without (right) solute return flow. In the central column, observed relative salinities are shown for 1990 and 2001 as qualitative comparison. The gray areas indicate the zones with relative concentrations between 0.01 and 0.2. The cross-sections show the mass distribution for both simulation scenarios: (1a) mass distribution just after the 10 days solute mass return flow, and (1b) after another 355 days of simulation without return flow and for the simulation scenario without mass return flow (2c) at the end of the 20-year simulation period. The graph shows the well-solute mass accumulation, which was calculated at the end of each year and re-introduced into the model in the following year.

the unsaturated zone can only be flushed when percolation takes place. However, it is not known whether the delay is longer than a year, or not. The aim was to provide long-term mass-conservation and not to simulate the physical processes taking place within the unsaturated zone.

4.2. Results from transient transport simulations for two scenarios (with and without salt recycling)

As already emphasised, neither the flow nor transport parameters were validated, and therefore the results of the two scenarios have to be compared relative to each other in the first place. Comparison with the real situation can only be done qualitatively, since the model reflects a conceptual hydrogeological model only.

Fig. 8 shows the results of the transport simulations with and without mass return flow from irrigation. The spreading of the low concentration iso-contours can be observed in the simulations with mass return flow, whereas the transition zone remains narrow in the simulations without mass return flow. Between the two simulation results the relative mass distribution as observed in the field is shown for the years 1990 and 2001 for visual comparison. It shows that, even though the absolute values simulated with the scenario with solute mass return flow are too low, the distribution and particularly the spreading of the iso-contours in the lower concentration range are in better accordance with reality than results from the scenario without mass return flow. In cross-section BB′, one can see that the introduced mass, which is visible in the top layers after the 10 days input period, disappears at the end of the year due to dilution, whereas the opposite effect is seen in cross-sections AA′. Cross-section AA′ having a thickness of only approximately 20% of cross-section BB′ does not allow as much dilution of the recycled solute mass. This shows, that differences in aquifer characteristics, such as saturated thickness, will influence the degree of salinisation.

Fig. 9a shows the comparison between the simulated concentrations of the two scenarios. The points on the correlation line represent the observation wells situated within the active seawater intrusion zone. The observation wells located far away of the correlation line are the observation points situated in the central area. For several of these points the simulated relative concentrations are lower than 10^{-4} for the scenario with $r_r = 0$, whereas for the scenario with solute recycling ($r_r = 1$) the relative concentrations are found to lie between 10^{-3} and 10^{-1}. This shows the impact of solute mass recycling on the spatial salinity distribution, as it is the only process, which is different between the two scenarios. Fig. 9b and c show the comparison between the observed and simulated relative concentrations at the end of the 20-year period for the two scenarios. As mentioned before, the comparison between the observed and simulated relative concentrations is qualitative. The graphs in Fig. 9b and c allow the identification of the observation wells in the central area relative to the ones situated in the seawater domain. For the scenario without mass return flow (Fig. 9b), all the observation wells placed inland are situated very far from the correlation line, whereas some of the observation wells are in good agreement with the measured concentrations, reflecting the observation points which are located within the effective seawater intrusion domain. For the scenario with solute mass return flow (Fig. 9c), a better correlation of the low relative concentrations is obtained (note that we are dealing with a logarithmic scale). Compared to Fig. 9b, the shifted values correspond to the observation wells situated in the central area of the aquifer which are not directly affected by the seawater intrusion. There, salinisation is likely to be dominated by solute mass return flow from irrigation.

5. Discussion

For the Kiti aquifer the evaluation of the relative impact of solute recycling from irrigation by means of the simplified solute mass balance approach led to an estimation of 1.5–8.5% of the extracted solute mass originating from recycling after a time-span of 20 years. These numbers are interesting because they seem to be small on the considered time-scale and one could be tempted to interpret them as reflecting a minor phenomenon. However, this amount seems to be sufficient to lead to groundwater degradation below a large part of the surface in the central area, where the aquifer thickness is small (Fig. 8), and can therefore have a high impact on agriculture. Furthermore, in

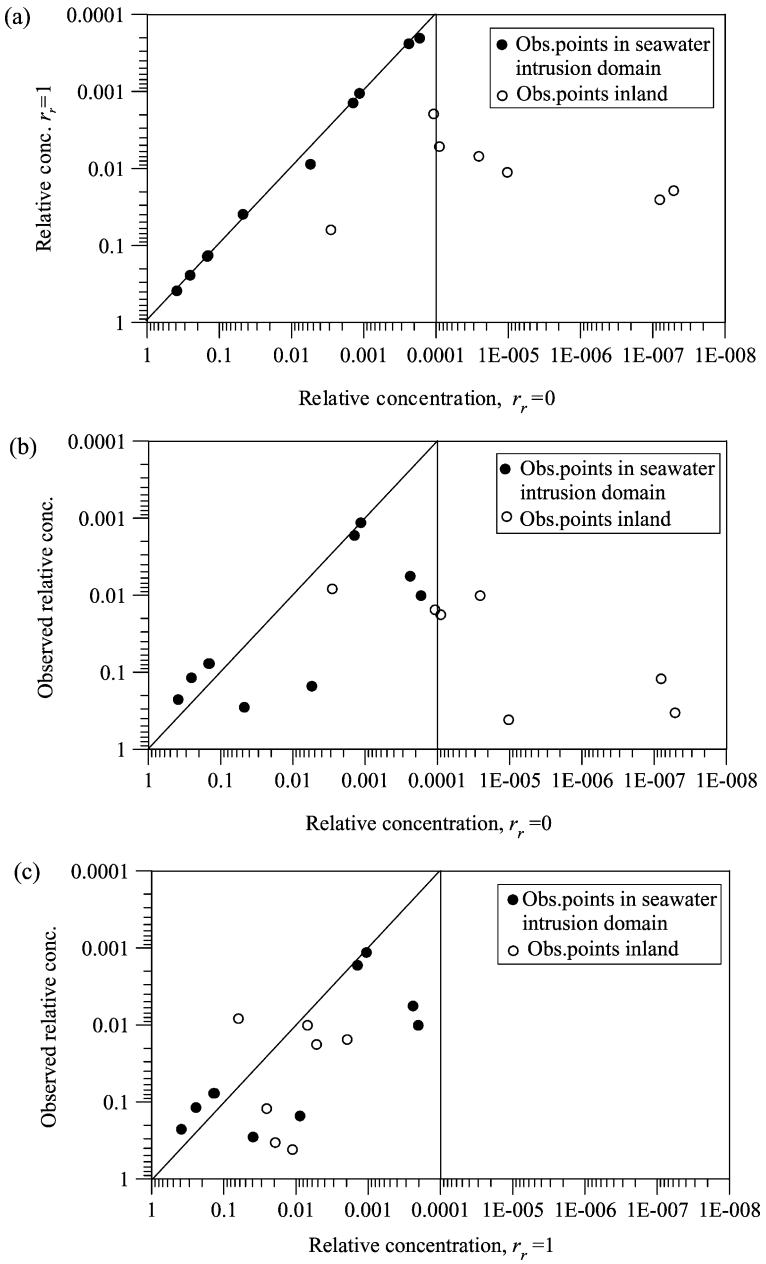

Fig. 9. Correlation between measured and simulated relative salinities as obtained at the end of the 20-year simulation periods with and without mass return flow from irrigation: (a) compares the results of the two simulated scenarios. The observation points located on the correlation line (black dots) are located within the active seawater intrusion domain, whereas the observation points inland (white dots) are characterised by relative concentrations below 10^{-4} for the scenario $r_r = 0$; (b) shows results from scenario without mass return flow ($r_r = 0$) compared to relative observed salinities, revealing a prominent scatter; (c) shows the comparison of the scenario with return flow ($r_r = 1$) with relative observed salinities and reveals that the simulated concentrations for the observation points inland (white dots) are within the zone of 'measureable' salinities. Thus, introducing mass return flow into the model widens the mixing zone.

the long term, recycling will considerably accelerate the deterioration of groundwater quality of the aquifer. The only brake to the acceleration is that the wells are eventually abandoned when a certain threshold concentration is attained. This fact was neither considered in the solute budget nor in the transient transport simulations.

The results from the 3D density-dependent flow and transport model indicated that mass return flow can explain the large spreading of the transition zone between fresh and seawater within an aquifer, depending on where solute recycling takes place. The main interest of this modelling approach lies in revealing the impact of the aquifer geometry, extraction and solute re-distribution pattern on the spatial salinity distribution, when solute recycling from irrigation is included in the simulations.

Using the simplified mass balance calculations in a pre-processing stage of numerical modelling can be a useful supplementary tool. The simplified solute mass balance approach is a quick and simple way of estimating whether solute recycling can be neglected with the mere knowledge of the return flow ratio r_r and the mean system turnover time t_0. However, it does not give any indications on the impact of solute recycling on the spatial salinity distribution and can therefore by no means substitute transport simulations.

Many assumptions were made within the mass balance calculations, as for instance the definition and use of a mean system concentration for the solute mass budget approach, which is the opposite characteristic of real coastal aquifers. However, by assuming that the extracted fluid has a mean system concentration, the potential danger can be formulated. Whether this hypothesis is reasonable or not can be evaluated by estimating whether the average extracted solute concentration is representative of the mean system concentration. This would be the case if extraction wells with similar discharge rates are homogeneously distributed over the whole aquifer. However, as an example, if extraction wells are situated far inland within the pure freshwater domain and the impact of solute recycling is evaluated for a time-span shorter than the time it takes for the wells to become affected by seawater intrusion, then the impact will be over-estimated. Another drawback is that the physics and chemistry of the salt recycling were not considered, and neither were the processes taking place within the unsaturated zone (adsorption, precipitation, dissolution, etc.). We simply assured that the salt mass balance was respected.

Possible other salinisation sources, such as salinisation from water–rock interactions within the bedrock formations and leaching into the base of the unconfined aquifer, were neglected but can be added at any time. As the purpose of this study was to investigate the possible impact of solute return flow from irrigation, no other salinity sources were incorporated.

Keeping the limitations of our models in mind, we would still like to emphasize the potential importance of solute mass return flow in coastal aquifers, as it is very likely to be a wide-spread phenomenon in many over-exploited irrigated coastal plains, not only in the Mediterranean area. Furthermore, it seems that up to now, most of the published groundwater flow and transport models in coastal aquifers have neglected solute mass return flow and might therefore have provided too optimistic forecasts. In view of sustainable groundwater exploitation in semi-arid coastal aquifers, the possible impact of salt recycling should be evaluated as an additional salinisation mechanism, directly coupled to seawater intrusion.

6. Conclusions

To investigate and quantify the impact of solute recycling from irrigation relative to seawater intrusion in over-exploited coastal aquifers, a simplified solute mass budget approach was established, allowing decomposition of the overall salinity extracted from wells into a contribution from the sea and a contribution from solute recycling. The transient solution for the relative contribution from solute recycling yielded a negative exponential function of the normalised time $\bar{t}$ (time t normalised with the system turnover time t_0) and the return flow ratio r_r, valid for any system, for which the specified hypotheses can be made.

Using the established simplified solute mass balance approach the relative impact of solute recycling was evaluated for an example from Cyprus, the Kiti aquifer. Field observations and analysis of

historical data suggested that the effect of solute mass return flow from irrigation is superimposed on the salinisation mechanism of seawater intrusion. The solute mass budget approach suggested that after 20 years 1.5–8.5% of the total extracted solute mass flux originates from recycling, for an estimated average system porosity range of 8–20%.

Numerical transport simulations were then carried out for a 20-year period, for two solute return flow ratios ($r_r = 0$: classical numerical approach, and $r_r = 1$: full solute mass return flow from irrigation), to investigate the impact of solute recycling on the spatial salinity distribution using a finite element model, which reflected the main hydrodynamic characteristics of the Kiti aquifer. The results were compared relative to each other and showed that the spatial salinity distributions obtained with $r_r = 1$ led to a spreading of the mixing zone in the central area, similar to what has been observed in the field, whereas the simulation without solute mass return flow revealed a very narrow transition zone at the end of the 20-year simulation period.

The interest of the simplified solute mass balance approach lies in the decomposition of the extracted solute mass flux into a component related to solute recycling and another component connected to seawater intrusion. It can be used if the return flow ratio r_r, the mean system turnover time t_0 and a characteristic time t can be estimated. This approach is thus a useful tool in a pre-processing stage of time-consuming numerical transport simulations to evaluate if solute recycling can be neglected or if it should be incorporated in the simulation procedure.

The advantage of transient transport simulations, on the other hand, lies in the capacity to reflect the impact of extraction/recharge and recycling patterns and aquifer geometry (e.g. aquifer thickness influencing dilution of recycled solute) etc. on the spatial salinity distribution but can only do this reliably, if the sources of groundwater contamination have been well defined. Hence, if solute return flow is important, then the salinity distribution cannot be simulated with a classical numerical approach ($r_r = 0$). A future objective is therefore to implement the solute mass return flow in a numerical tool as coupled boundary condition and to link it to the physical processes taking place within the unsaturated zone.

As soon as a clear spatial distinction can be made between seawater intrusion and solute mass return flow, the salinisation risk potential towards the coupled salinisation mechanisms can be defined, and with it, the different potential remedial measures.

Acknowledgements

This work was financially supported by the European Commission: Research Project BBW 97.0621. We would like to thank the Cyprus Water Development Department, in particular Dr A. Christodoulides, for providing field assistance and historical data, and for fruitful discussions.

References

Bear, J., Cheng, A.H.-D., Sorek, S., Ouazar, D., Herrera, I., 1999. Seawater Intrusion in Coastal Aquifers: Concepts, Methods and Practices. Kluwer, Dordrecht.

Beke, G.J., Entz, T., Graham, D.P., 1993. Long-term quality of shallow groundwater at irrigated sites. Journal of Irrigation and Drainage Engineering, ASCE 119 (1), 116–128.

Bouwer, H., 1987. Effect of irrigated agriculture on groundwater. Journal of Irrigation and Drainage Engineering, ASCE 113 (1), 4–15.

Close, M.E., 1987. Effects of irrigation on water-quality of a shallow unconfined aquifer. Water Resources Bulletin 23 (5), 793–802.

Diersch, H.-J., 1998. FEFLOW Reference Manual. WASY Institute for Water Resources Planning and Systems Research, Berlin.

El Achheb, A., Mania, J., Mudry, J., 2001. Processus de salinisation des eaux souterraines dans le basin Sahel-Doukkala (Maroc occidental), First International Conference on Saltwater Intrusion and Coastal aquifers- Monitoring, Modeling and Management, Essaouira, Morocco,.

Essaid, H.I., 1990. A multilayered sharp interface model of coupled freshwater and saltwater flow in coastal systems: model development and application. Water Resources Research 26 (7), 1431–1454.

Frind, E.O., 1982. Seawater intrusion in continuous coastal aquifer-aquitard systems. Advances Water Resources 5, 89–97.

Gambolati, G., Putti, M., Paniconi, C., 1999. Three-dimensional model of coupled flow and miscible salt transport. In: Bear, J., Cheng, A.H.-D., Sorek, S., Ouazar, D., Herrera, I. (Eds.), Seawater Intrusion in Coastal Aquifers: Concepts, Methods and Practices, Kluwer, Dordrecht, (Chapter 10).

Gordon, E., Shamir, U., Bensabat, J., 2000. Optimal management of a regional aquifer under salinization conditions. Water Resources Research 36 (11), 3193–3203.

Höltin, B., 1996. Hydrogeologie: Einführung in die Allgemeine und Angewandte Hydrogeolgogie, 5. Auflage. Ferdinand Enke Verlag, Stuttgard.

Hsü, K.J., Ryan, W.B.F., Cita, M.B., 1973. Late Miocene desiccation of the Mediterranean. Nature 20 (242), 240–244.

Jackovides, J., 1982. Southern Conveyor Project, Feasibility Study, Groundwater Resources, vol. 3. Cyprus Water Development Department, Nicosia.

Johannsen, K., Kinzelbach, W., Oswald, S., Wittum, G., 2002. The saltpool benchmark problem-numerical simulation of saltwater upconing in a porous medium. Advances in Water Resources 25 (3), 335–348.

Kim, Y., Lee, K.S., Koh, D.C., Lee, D.H., Lee, S.G., Park, W.B., Koh, G.W., Woo, N.C., 2003. Hydrogeochemical and isotopic evidence of groundwater salinisation in a coastal aquifer: a case study in Jeju volcanic island, Korea. Journal of Hydrology 270, 282–294.

Kolodny, Y., Katz, A., Starinsky, A., Moise, T., Simon, E., 1999. Chemical tracing of salinity sources in Lake Kinneret (Sea of Galilee), Israel. Limnology and Oceanography 44 (4), 1035–1044.

Konikow, L.F., Person, M., 1985. Assessment of long-term salinity changes in an irrigated stream-aquifer system. Water Resources Research 21 (11), 1611–1624.

Oude Essink, G.H.P., 2001. Salt water intrusion in a three-dimensional groundwater system in the Netherlands: a numerical study. Transport in Porous Media 43, 137–158.

Paniconi, C., Khalifi, I., Lecca, G., Giacomelli, A., Tarhouni, J., 2001. Modeling and analysis of seawater intrusion in the coastal aquifer of Eastern Cap-Bon, Tunisia. Transport in Porous Media 43, 3–28.

Pearce, M.W., Schumann, E.H., 2001. The impact of irrigation return flow on aspects of the water quality of the Upper Gamtoos Estuary, South Africa. Water SA 27 (3), 367–372.

Ploethner, D., Avramadis, C., Charalambidis, A., Geyh, M.A., Schmidt, G., Wagner, W., Zomenis, S., 1986. Hydrochemistry and quality problems of groundwater in the Kiti area, Project Report Hydrochemistry, Technical Cooperation Cyprus–German Geological and Pedological Project (Nr. 81.222.4), Bundestanstalt für Geowissenschaften und Rohstoffe, Hannover.

Prendergast, J.B., Rose, C.W., Hogarth, W.L., 1993. Sustainability of conjunctive water use for salinity control in irrigated areas: theory and application to the Shepparton region, Australia. Irrigation Science 14, 177–187.

Schmidt, G., Ploethner, D., Avraamadis, C., Wagner, W., Zomenis, S., 1988. Technical Cooperation Cyprus–German Geological and Pedological Project, Groundwater Model Investigation on the Kiti Aquifer, Bundestanstalt für Geowissenschaften und Rohstoffe, Hannover.

Sherif, M., Hamza, K., 2001. Mitigation of seawater intrusion by pumping brackish water. Transport in Porous Media 43, 29–44.

Sites, W., Kraft, G.J., 2000. Groundwater quality beneath irrigated vegetable fields in a north-central US sand plain. Journal of Environmental Quality 29 (5), 1509–1517.

Strigter, T.Y., Van Ooijen, S.P.J., Post, V.E.A., Appelo, C.A.J., Carvahlo Dill, A.M.M., 1998. A hydrogeological and hydrochemical explanation of the groundwater composition under irrigated land in a Mediterranean environment, Algarve, Portugal. Journal of Hydrology 208, 262–279.

Vengosh, A., Rosenthal, E., 1994. Saline groundwater in Israel: its bearing on the water crisis in the country. Journal of Hydrology 156, 389–430.

Vengosh, A., Spivack, A., Artzi, Y., Avner, A., 1999. Geochemical and boron, strontium and oxygen isotopic constraints on the origin of the salinity in groundwater from the mediterranean coast of Israel. Water Resources Research 35 (6), 1877–1894.

Vengosh, A., Gill, J., Davisson, M.L., Hudson, G.B., 2002. A multi-isotope (B, Sr, O, H and C) and age-dating (H-3, He-3 and C-14) study of groundwater from salinas Valley, California: hydrochemistry, dynamics and contamination processes. Water Resources research 38 (1) art No. 1008.

Voss, C.I., 1999. USGS SUTRA code-history, practical use, and application in Hawaii. In: Bear, J., Cheng, A.H.-D., Sorek, S., Ouazar, D., Herrera, I. (Eds.), Seawater Intrusion in Coastal Aquifers: Concepts, Methods and Practices, Kluwer, Dordrecht, (Chapter 9).

Xue, Y., Chunhong, X., Wu, J., 1995. A three-dimensional miscible transport model for seawater intrusion in China. Water Resources Research 31 (4), 903–912.